Vol 18 No 7, July 2009
1674-1056/2009/18(07)/3090-09

Chinese Physics B

© 2009 Chin. Phys. Soc.
and IOP Publishing Ltd

Numerical method of studying nonlinear interactions between long waves and multiple short waves*

Xie Tao(谢 涛)[a)†], Kuang Hai-Lan(旷海兰)[a)], William Perrie[b)], Zou Guang-Hui(邹光辉)[a)], Nan Cheng-Feng(南撑峰)[a)], He Chao(何 超)[a)], Shen Tao(沈 涛)[a)], and Chen Wei(陈 伟)[a)]

[a)] *School of Information Engineering, Wuhan University of Technology, Wuhan 430070, China*

[b)] *Bedford Institute of Oceanography, B2Y 4A2, Dartmouth, NS, Canada*

(Received 14 December 2008; revised manuscript received 30 December 2008)

Although the nonlinear interactions between a single short gravity wave and a long wave can be solved analytically, the solution is less tractable in more general cases involving multiple short waves. In this work we present a numerical method of studying nonlinear interactions between a long wave and multiple short harmonic waves in infinitely deep water. Specifically, this method is applied to the calculation of the temporal and spatial evolutions of the surface elevations in which a given long wave interacts with several short harmonic waves. Another important application of our method is to quantitatively analyse the nonlinear interactions between an arbitrary short wave train and another short wave train. From simulation results, we obtain that the mechanism for the nonlinear interactions between one short wave train and another short wave train (expressed as wave train 2) leads to the energy focusing of the other short wave train (expressed as wave train 3). This mechanism occurs on wave components with a narrow frequency bandwidth, whose frequencies are near that of wave train 3.

Keywords: sea surface, nonliear interaction, numerical method
PACC: 9210D, 9210H

1. Introduction

Wave–wave interactions in infinitely deep water have been studied during the last century by using theoretical and numerical methods. For example, with the inverse scattering transform (IST) method, Chow *et al* [1] obtained a theoretical formulation for the nonlinear three-wave interactions describing the saturation of one unstable wave coupled to two damped waves. Additional pioneering studies include four-wave interactions by Phillips,[2] which is based on Zakharov's equation[3] for the temporal evolution of the complex amplitude function for wave spectra, five-wave interactions[4−7] and four-wave interactions.[8] A quantitative model was developed to examine the evolution of ratio between the growth rate and the total energy density of wind waves affected by long waves.[9] Besides the interaction between a unidirectional deep-water short wave train and an intermediate-depth long wave,[10,11] the 2-D weak interactions of solitons in shallow water have also been investigated by using theoretical methods.[12] Recently, the Hamiltonian formalism was used to represent wave–wave interactions and a new type of modulation instability.[13]

Meanwhile, numerical methods to study the wave–wave interactions have also been developed. Lo and Chiang[14] developed a standard split-step, pseudo-spectral Fourier method to study water-wave modulation. A numerical method of studying surface hydrodynamics including long wave–short wave interactions was earlier studied by West *et al.*[15] A higher order (second and third orders) hydrodynamic modulation transfer function (MTF) was presented by Tanos *et al.*[16] To better understand radar images of sea waves with water wavelengths longer than the radar range resolution, Pan and Johnson[17] investigated the modulation of short waves by longer waves using the numerical method. In the cubic spline

*Project supported by the National High Technology Research and Development Program of China (Grant No 2007AA12Z170), the Major Research Plan of the National Natural Science Foundation of China (Grant No 40706058) , the Science-Technology Chenguang foundation for Young Scientist of Wuhan, China (Grant No 200850731388), and the Canadian Space Agency Government Related Initiatives Program (GRIP) entitled Building Satellite Data into Fisheries and Oceans Operational Systems.

†Corresponding author. E-mail: xtplqk@whut.edu.cn

approximation, Sriram *et al* [18] developed a finite element method to simulate 2-D nonlinear waves. A quadratic higher order boundary element model with a channel Green's function was developed by Ning *et al* [19] and used to simulate nonlinear regular and focused waves in infinitely deep water.

Although many studies have been carried out on wave–wave interactions in deep water, less attention has been paid to the problem of nonlinear interactions between a long wave and multiple short harmonic waves. It is recognized that the short gravity water waves are nonlinearly modulated by long waves when short waves ride on the long wave. Unna[20−22] first pointed out that short waves were shortened at the crests of the long waves and lengthened in the troughs, for example, when gravity waves of fairly short wavelengths rode on the surfaces of much longer waves, such as tidal currents or ocean swell.[20−22] Taking into account the nonlinear interactions between the two wave trains, Longuet–Higgins and Stewart[23] calculated the changes in wavelength and amplitude of the shorter wave train in infinitely deep water. The wave–number and the amplitude for a short harmonic wave that is modulated by a long wave can be expressed as

$$k' = k_1 \left(1 + a_2 k_2 \sin \psi_2\right), \tag{1}$$

and

$$a' = a_1 \left(1 + a_2 k_2 \sin \psi_2\right), \tag{2}$$

where $kx - \sigma t + \theta = \psi$; a, k, σ denote the wave amplitude, the wave–number and the frequency respectively; subscripts (1,2 ...) indicate the serial number of waves. Here, 1 denotes a long wave, and 2 refers to the short wave, after Longuet–Higgins and Stewart.[23]

The interaction between short and long waves is an important component in the remote sensing of ocean surface winds. Using linear ocean wave theory, linear ocean wind surface models have been established (e.g. in Refs.[24–26]) based on assumed ocean wave spectra, for example, the Pierson–Moskowitz spectrum[27] or the JONSWAP spectrum described by Hasselmann *et al.*[28] However, the sea surface is nonlinear, where different harmonic waves interact nonlinearly with one another. These interactions can cause the sea surface roughness to change. It is therefore necessary to consider the nonlinear interactions between long waves and multiple harmonic short waves because remote sensors are especially sensitive to sea surface roughness.

What will happen to the nonlinear interactions between a given long wave and multiple short harmonic waves when the number of harmonic short waves is increased? It is difficult to solve this problem by using the analytical methods available from existing studies because the boundary conditions cannot be solved analytically when more than two short waves ride on a long wave. The purpose of this paper is to present a new numerical method to study nonlinear interactions between a long wave and multiple short harmonic waves in infinitely deep water.

2. General basis of numerical method

To simplify the numerical calculations, the definitions of subscripts 1 and 2 in the present paper are the opposite to those given by Longuet–Higgins and Stewart.[23] We define subscript 1 as the long wave, while the serial numbers (2,3,... n) denote corresponding short harmonic waves; for example 2 denotes the first short wave, 3 denotes the second short wave, and so on.

The ocean wave hydrodynamics equations are

$$\boldsymbol{u} = \nabla \phi, \tag{3a}$$

$$\nabla^2 \phi = 0, \tag{3b}$$

$$\frac{p}{\rho} + gz + \frac{1}{2}\boldsymbol{u}^2 + \frac{\partial \phi}{\partial t} = 0, \tag{3c}$$

where $\boldsymbol{u}$, g, p, ρ, and ζ denote the velocity, the gravity accelerate, the pressure, the density and the surface elevation, respectively. When a short wave is perturbed by a long wave (the assumed limitation of perturbation method is $k_2 >> k_1$), expansion parameters can be expressed as

$$\boldsymbol{u} = \boldsymbol{u}^{(0)} + \varepsilon \mathbf{u}^{(1)} + \dots, \tag{4a}$$

$$\phi = \phi^{(0)} + \varepsilon \phi^{(1)} + \dots, \tag{4b}$$

$$\zeta = \zeta^{(0)} + \varepsilon \zeta^{(1)} + \dots, \tag{4c}$$

and

$$\frac{p}{\rho} + gz = p^{(0)} + \varepsilon p^{(1)} + \dots. \tag{4d}$$

The wave-number and the amplitude for short harmonic wave 2, which is modulated by long wave 1, can be expressed analytically. Thus, the surface evolution

of the system is[23]

$$\zeta_{12} = \left(a_1 \sin\psi_1 - \frac{1}{2}a_1^2 k_1 \sin(2\psi_1)\right) + \left(a_2 \sin\psi_2 - \frac{1}{2}a_2^2 k_2 \sin(2\psi_2)\right) - a_1 a_2 (k_1 \cos\psi_1 \cos\psi_2 - k_2 \sin\psi_1 \sin\psi_2). \tag{5}$$

Before introducing the numerical method, we present the following concepts:

(1) A given wave 1 can be considered as a 'nonlinear long wave' when a short wave 2 (or several short harmonic waves) rides on long wave 1. These nonlinear long waves can be denoted by subscripts 12 or 123, 1234 *et al*. Parameters with subscript 12 denote those of the nonlinear long wave 12 when the first short wave 2 rides on long wave 1. Parameters with subscript 12 denote those of the nonlinear long wave 123 when the second short wave 3 rides on the nonlinear long wave 12. Additional interactions are labeled by analogy.

(2) Frequencies, amplitudes and wave numbers are variable. Nonlinear long waves can be regarded as waves whose frequencies, amplitudes and wave numbers vary temporally and spatially.

(3) A given nonlinear long wave can be considered to be discrete; there is a corresponding amplitude and wave number at every temporal and spatial point. The surface elevation of the nonlinear long wave at a given location can be regarded as a corresponding surface elevation of a sine wave whose amplitude and wave number are those of the long wave at that point.

(4) Discrete interactions are assumed to exist between a nonlinear long wave and short waves. The result of interactions between a nonlinear long wave and short waves can be regarded as the sum of interactions between short waves and different sine waves whose amplitudes and wave–numbers are equal to those of the nonlinear long wave at different points.

2.1. Surface elevations of two short waves riding on a long wave

Firstly, we consider the interactions between long wave 1 and short wave 2. The surface elevation of nonlinear long wave 12 can be derived and given as expression (5). The variable amplitude and wave–number are

$$a_{12} = a_1(1 + a_2 k_2 \sin\psi_2), \tag{6}$$

and

$$k_{12} = k_1(1 + a_2 k_2 \sin\psi_2), \tag{7}$$

and the frequency satisfies the dispersive relation

$$\sigma_{12} = \sqrt{g k_{12}}. \tag{8}$$

Secondly, ζ_{12} is regarded as the surface elevation of nonlinear long wave 12. ζ_{123} denotes the surface elevation of the system in which short wave 3 rides on nonlinear long wave 12.

At a certain spatial point i and temporal point j, namely (i, j), the surface elevation of the discrete nonlinear long wave is

$$\zeta_{(12,i,j)} = a_{(12,i,j)} \sin\psi_{(12,i,j)}, \tag{9}$$

where $\psi_{(12,i,j)} = k_{(12,i,j)} x_i - \sigma_{(12,i,j)} t_j + \theta_{(12,i,j)}$, $\theta_{(12,i,j)}$ can be calculated by $\zeta_{(12,i,j)} = \zeta_{12}\big|_{x=x_i,t=t_j}$. At point$(i, j)$, we extend $\zeta_{(12,i,j)}$ to the whole time–space domain

$$\zeta_{12} = a_{12} \sin\psi_{12}, \tag{10}$$

and we note that at a different point, there is a corresponding different sine wave equation. The problem where short wave 3 rides on long wave 12 can be easily solved by using the method of Longuet–Higgins and Stewart.[23] It can be expressed as

$$\zeta_{(123,i,j)} = \zeta_{123}^{(0)}\big|_{x=x_i,t=t_j} + \zeta_{(123,i,j)}^{(1)}, \tag{11}$$

where

$$\zeta_{123}^{(0)} = \left(a_1 \sin\psi_1 - \frac{1}{2}a_1^2 k_1 \sin(2\psi_1)\right) + \left(a_2 \sin\psi_2 - \frac{1}{2}a_2^2 k_2 \sin(2\psi_2)\right) - a_1 a_2 (k_1 \cos\psi_1 \cos\psi_2 - k_2 \sin\psi_1 \sin\psi_2) + \zeta_3, \tag{12}$$

and

$$\zeta_{(123,i,j)}^{(1)} = -\frac{1}{2}a_3^2 k_3 \sin(2\psi_3) - \frac{1}{2}a_{12}^2 k_{12} \sin(2\psi_{12}) - a_{12}a_3(k_{12} \cos\psi_{12} \cos\psi_3 - k_3 \sin\psi_{12} \sin\psi_3)\big|_{x=x_i,t=t_j} \tag{13}$$

with $\zeta_3 = a_3 \sin\psi_3$ and $\psi_3 = k_3 x - \sigma_3 t + \theta_3$.

Finally, surface elevation of system 123 is given by sets of equations following expression (11):

$$\zeta_{123}\big|_{x=x_i,t=t_j} = \zeta_{(123,i,j)}$$
$$x,t \in \{-\infty < x_i < \infty,\quad 0 \le t_i < \infty\}. \tag{14}$$

2.2. Surface elevations of n short waves riding on a long wave

When the nth short wave rides on a nonlinear long wave $12\ldots n-1$, we let $\zeta_{12\ldots n-1}$ denote the surface elevation of nonlinear long wave $12\ldots n-1$. Therefore $\zeta_{12\ldots n}$ denotes the surface elevation of the nonlinear wave when the nth short wave is modulated by nonlinear long wave $12\ldots n-1$.

Its parameters are

$$a_{12\ldots n} = a_{12\ldots n-1}(1 + a_n k_n \sin\psi_n)\big|_{x=x_i,t=t_j}, \tag{15a}$$
$$k_{12\ldots n} = k_{12\ldots n-1}(1 + a_n k_n \sin\psi_n)\big|_{x=x_i,t=t_j}, \tag{15b}$$

and

$$\sigma_{12\ldots n} = \sqrt{g k_{12\ldots n}}\big|_{x=x_i,t=t_j}. \tag{15c}$$

At point (i,j), the surface elevation of the discrete nonlinear long wave can be expressed as a sine wave

$$\zeta_{(12\ldots n,i,j)} = a_{(12\ldots n,i,j)} \sin\psi_{(12\ldots n,i,j)}, \tag{16}$$

where $\psi_{(12\ldots n,i,j)} = k_{(12\ldots n,i,j)}x_i - \sigma_{(12\ldots n,i,j)}t_j + \theta_{(12\ldots n,i,j)}$and $\theta_{(12\ldots n,i,j)}$ is derived from $\zeta_{(12\ldots n,i,j)} = \zeta_{12\ldots n}\big|_{x=x_i,t=t_j}$.

We re-express $\zeta_{(12\ldots n,i,j)}$ as

$$\zeta_{12\ldots n} = a_{12\ldots n}\sin\psi_{12\ldots n}\big|_{x=x_i,t=t_j}$$
$$x,t \in \{-\infty < x_i < \infty,\quad 0 \le t_j < \infty\}. \tag{17}$$

At a different spatial-temporal point, there is a correspondingly different sine wave equation. We can regard the nonlinear wave surface elevation $\zeta_{12\ldots n}$ as the result of different nonlinear interactions between every extended long wave $12\ldots n-1$ $(x = x_i, t = t_j)$ and nth short wave. The effect of the nth short wave riding on nonlinear long wave $12\ldots n-1$ can be investigated easily. It can be expressed as

$$\zeta_{(12\ldots n,i,j)}\big|_{x=x_i,t=t_j} = \zeta^{(0)}_{12\ldots n}\big|_{x=x_i,t=t_j} + \zeta^{(1)}_{(12\ldots n,i,j)}\big|_{x=x_i,t=t_j}, \tag{18}$$

$$\zeta^{(0)}_{12\ldots n}\big|_{x=x_i,t=t_j} = \zeta_{12\ldots n-1}\big|_{x=x_i,t=t_j} + \zeta_n\big|_{x=x_i,t=t_j}, \tag{19}$$

and

$$\begin{aligned}\zeta^{(1)}_{(12\ldots n,i,j)}\big|_{x=x_i,t=t_j} = {} & -\frac{1}{2}a_n^2 k_n \sin(2\psi_n)\big|_{x=x_i,t=t_j} - \frac{1}{2}a^2_{12\ldots n-1}k_{21\ldots n-1}\sin(2\psi_{12\ldots n-1})\big|_{x=x_i,t=t_j} \\ & - a_{12\ldots n-1}a_n(k_{12\ldots n-1}\cos\psi_{12\ldots n-1}\cos\psi_n - k_n\sin\psi_{12\ldots n-1}\sin\psi_n)\big|_{x=x_i,t=t_j}\end{aligned} \tag{20}$$

where $\zeta_n = a_n \sin\psi_n$, and $\psi_n = k_n x - \sigma_n t + \theta_n$.

3. Application of the method

In this section, we use our new method to simulate several examples, i.e. the nonlinear waves resulting from the case where 1 to 6 short waves ride on a given long wave. Waves in our case are monochromatic waves. Assuming fully developed sea conditions for a given wind speed, we use the Pierson–Moskowitz spectral model[27] to determine the parameters for the long wave and all short waves. These parameters are shown in Table 1, namely amplitude, frequency, wavelength and initial phase.

Using our method, one can theoretically simulate nonlinear waves when many short waves ride on a given long wave. We present evolution diagrams for the sea surface elevation and frequencies in the temporal and spatial domains in Figs.1 and 2. Here, short wave 2 is modulated by long wave 1. Owing to nonlinear modulation as described by Longuet-Higgins and Stewart,[23] the amplitude and the wave number are maximal at crests and minimal at troughs. Moreover, these variables do not change at the zero level of the sea surface. The numerical simulation result (ζ_{12}) of short wave 2 modulated by long wave is coincided with the result in Ref.[23]. Similar modulation trend in x direction of multiple short waves modulated by long wave is shown in Fig.1. As demonstrated, our method is valid.

Table 1. Monochromatic wave parameters with the use of a Pierson–Moskowitz spectrum: long wave, short wave, wind speed, amplitude, frequency, wavelength, and initial phase, denoted by LW, SW, WS, A, F, WL, and IP respectively.

	LW	SW1	SW2	SW3	SW4	SW5	SW6
WS/(m/s)	15.00	3.00	1.60	4.10	5.30	3.70	4.50
A/m	2.40	0.09	0.02	0.18	0.30	0.14	0.21
F/Hz	0.09	0.46	0.86	0.33	0.26	0.37	0.30
WL/m	193.00	7.37	2.11	14.30	23.10	11.40	17.30
IP/(°)	75.0	137.0	282.0	245.0	166.0	204.0	286.0

We are also to determine the nonlinear interactions between long wave 1 and other short waves. But this cannot be directly found in Figs.1 and 2. However, subtracting linear wave elevation $(\zeta_1 + \zeta_2 + \ldots + \zeta_n)$ from the corresponding nonlinear wave elevation $\zeta_{12\ldots n}$, one can obtain the elevation difference caused by nonlinear interactions, i.e. $\Delta\zeta_{12\ldots n} = \zeta_{12\ldots n} - (\zeta_1 + \zeta_2 + \ldots + \zeta_n)$.

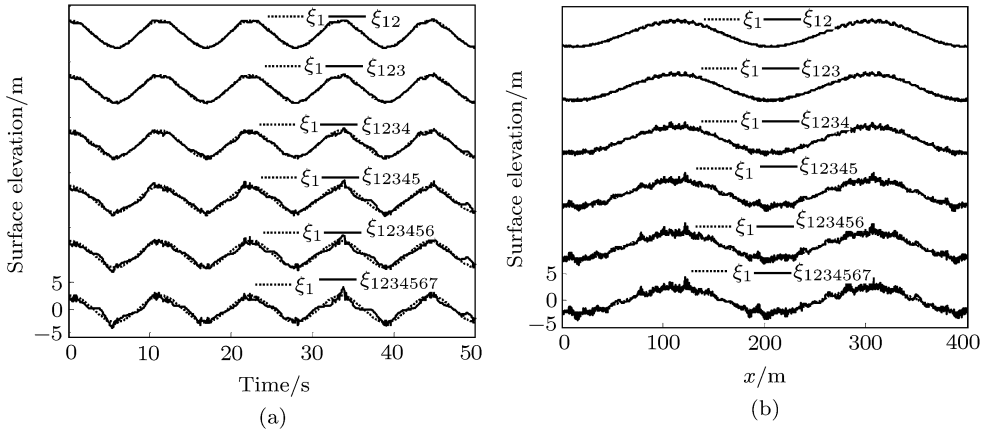


Fig.1. Comparison among the surface elevations of a nonlinear long wave as a function of time (a) and as a function of space (b).

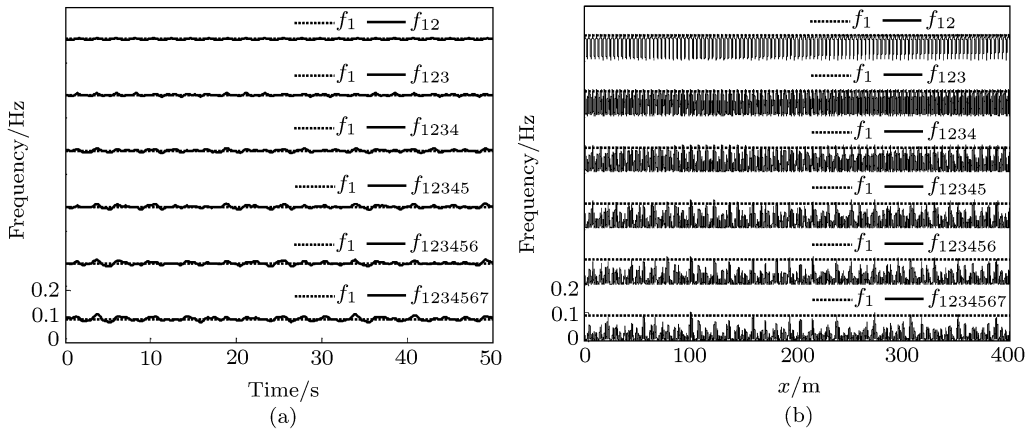


Fig.2. Evolutions of frequency of nonlinear long wave with time (a) and space (b) separately.

As an example, the differences in elevation among the cases in Fig.1(b) are shown in Fig.3(a), where zero level locations for long wave 1 are indicated by the vertical dot lines intersecting the ζ_1 contours. From Fig.3(a), one finds that the elevation difference becomes larger with the increase of the number of short waves at a given spatial point. This means that all the short waves are modulated by the nonlinear long wave. This can also be verified by Fig.3(b), which directly shows the evolution of the amplitude differences caused by

nonlinear interactions between the short wave and nonlinear surface elevation, where $\Delta\zeta_{12} = \zeta_{12} - (\zeta_1 + \zeta_2)$, $\Delta\zeta_{123} = \zeta_{123} - (\zeta_{12} + \zeta_3)$, ..., $\Delta\zeta_{12\ldots n} = \zeta_{12\ldots n} - (\zeta_{12\ldots n-1} + \zeta_n)$.

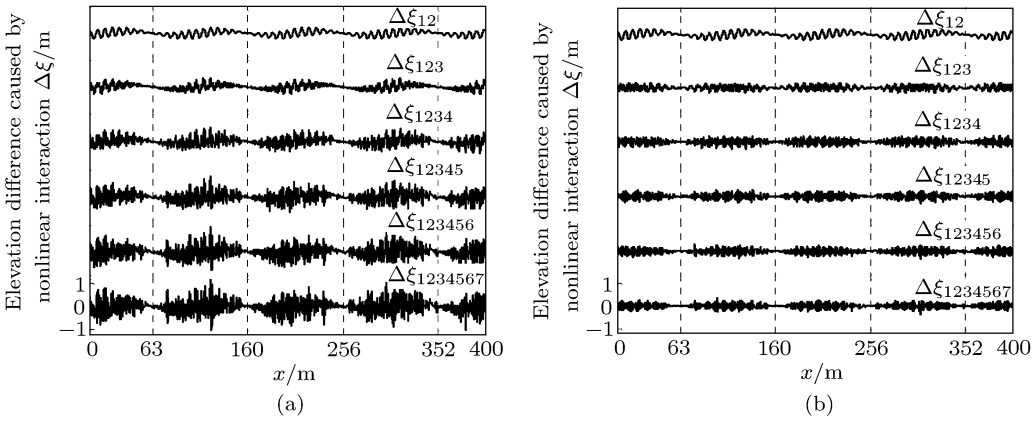


Fig.3. Evolution diagrams of amplitude differences (a) between linear and nonlinear surface elevations, where $\Delta\zeta_{12} = \zeta_{12} - (\zeta_1 + \zeta_2)$, $\Delta\zeta_{123} = \zeta_{123} - (\zeta_1 + \zeta_2 + \zeta_3), \ldots$, $\Delta\zeta_{12\ldots n} = \zeta_{12\ldots n} - (\zeta_1 + \zeta_2 + \ldots + \zeta_n)$; (b) caused by nonlinear interactions between short wave and nonlinear surface elevation, where $\Delta\zeta_{12} = \zeta_{12} - (\zeta_1 + \zeta_2)$, $\Delta\zeta_{123} = \zeta_{123} - (\zeta_{12} + \zeta_3), \ldots$, $\Delta\zeta_{12\ldots n} = \zeta_{12\ldots n} - (\zeta_{12\ldots n-1} + \zeta_n)$.

Is there any nonlinear interaction between one short wave train and another short wave train? In fact, this question induces another application of our new method, that is, it may be applied to the quantitative analysis of nonlinear interactions between a pair of arbitrary short wave trains. We consider the nonlinear interactions between short wave train 2 and short wave train 3. We first calculate the temporal evolution of surface elevation (ζ_1, ζ_{12}, ζ_{13}, ζ_{123}). Then we transform these temporal evolution diagrams into amplitude spectral space ($P_1(f)$, $P_{12}(f)$, $P_{13}(f)$, $P_{123}(f)$) with the Fast Fourier Transform intensity caused by the nonlinear interactions between short wave trains 2 and 3 at different frequencies, where,

$$\Delta P_{23}^{\mathrm{r}}(f) = (P_{123}(f) - (P_{12}(f) + P_{13}(f) - P_1(f)))/(P_1(f) + P_2(f) + P_3(f)). \tag{21}$$

Figure 4 shows the relative spectral intensity change between nonlinear wave spectral intensities: $P_{123}(f)$ and $(P_{12}(f) + P_{13}(f)) - P_1(f)$. In both cases, the long wave train (with subscript 1 and frequency 0.09Hz) is generated by wind at a speed of 15 m/s. In case (a), the first short wave train (with subscript 2) is generated by wind at a speed of 3 m/s. The second short wave train (with subscript 3) is generated by wind at a speed of 1.6 m/s. In case (b), the primary parameters for the short wave trains are the same as those of (a), but their sequences are exchanged, i.e. long wave train 1 first interacts with short wave train 3, then nonlinear long wave train 13 interacts with short wave train 2 (here, we do not change the subscripts). Changing parameter values of the long and the short wave trains from the cases of Fig.4, we can find a common phenomenon, that is, $\Delta P_{23}^{\mathrm{r}}(f)$ or $\Delta P_{32}^{\mathrm{r}}(f)$ changes occur mainly near the frequency of the short wave trains in all results. Thus, from these results we can answer the first question posed above; there exists a nonlinear interaction between one short wave train and another short wave train.

From Fig.4, it is obvious that energy focusing occurs for the short wave train 3. Notable spectral amplitude attenuation appears in several specific frequency bands, distributed over the frequency range, from low to high frequencies, while several selected spectral amplitudes are dramatically enhanced at other frequency bands, which are related to the attenuated frequency bands. We also perform numerous additional simulations, for example as shown in Fig.5, giving essentially the same results. Thus, the main characteristic of the nonlinear interactions between one short wave train and another short wave train is that the first short wave train experiences dramatic transfer of energy into the second short wave train, at selected frequencies. The locations of these frequencies are discussed next.

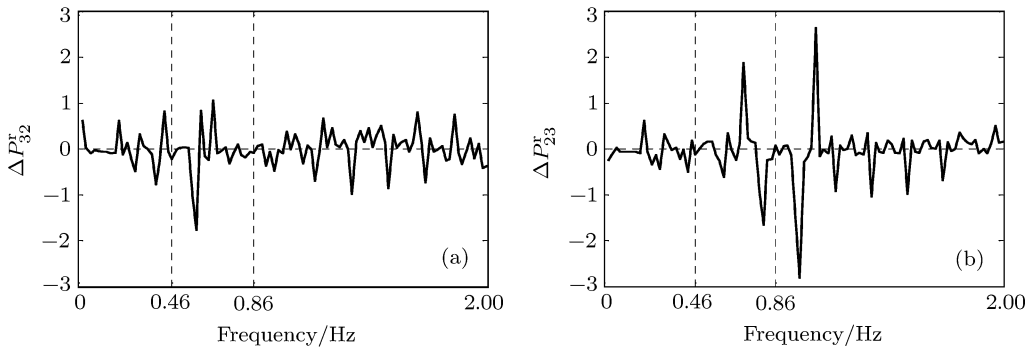


Fig.4. Relative spectrum intensity change between nonlinear wave spectrum intensity P_{123} and $(P_{12}+P_{13})-P_1$. In both cases, long wave train (index 1, frequency 0.09 Hz) is generated by the wind at a speed of 15 m/s, where panel (a) shows that the first short wave train (index 2) is generated by wind at a speed of 3 m/s, and the second short wave train (index 3) is generated by wind at a speed of 1.6 m/s and panel (b) exhibits that parameters of short wave trains are the same as those in panel (a), but their sequences are exchanged, i.e. long wave 1 first interacts with short wave train 3, then the nonlinear long wave train 13 interacts with short wave train 2.

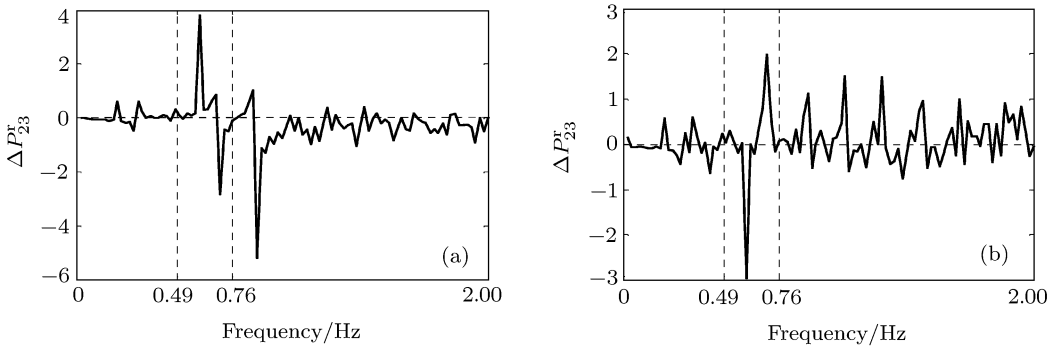


Fig.5. The same as in Fig.4, except that the first short wave train (labelled as 2) is generated by wind at a speed of 2.8 m/s, and the second short wave train (labelled as 3) is generated by wind at a speed of 1.8 m/s in panel (a).

Using our method, we can also quantitatively analyse the nonlinear interactions between an arbitrary short wave train and another short wave train. Figure 4(a) shows the nonlinear effects of short wave train 2 on short wave train 3. The primary frequencies of short wave trains 2 and 3 are 0.46 Hz and 0.86 Hz respectively. One can find that the peak value of $\Delta P^{\rm r}_{23}(f)$ (which is 2.63) appears at frequency 1.06 Hz. The second peak value of $\Delta P^{\rm r}_{23}(f)$ (which is 1.868) occurs at frequency 0.7 Hz. The two frequencies are close to the primary frequency of the short wave train 3, or rather, they are located on both sides of this primary frequency. There are two sharp 'troughs' or minima lying in the frequency band between the first peak frequency and the second peak frequency. The corresponding 'trough' values of $\Delta P^{\rm r}_{23}(f)$ and frequencies are (–1.667, 0.80 Hz), and (–2.818, 0.98 Hz) respectively. The result in Fig.4(a) means that the wave energy (or momentum) with a narrow frequency bandwidth and primary frequencies near 0.7 Hz and 1.06Hz is increased because of the nonlinear interactions between short wave trains 2 and 3. Because of conservation of energy, the spectral intensity increases from the two frequency 'trough' bands near 0.8 Hz and 0.98 Hz respectively. In Fig.4, we do not consider the spectral change when the frequencies are outside the span from 0.06 Hz to 1 Hz, because the absolute spectral intensity at these frequencies is much lower than the spectral intensity contained between 0.06 Hz and 1 Hz.

To study the nonlinear effect of short wave train 3 on short wave train 2, we first simulate nonlinear long wave train 13. We then consider how short wave train 3 acts on short wave train 2. Results similar to those in Fig.4(a) appear in Fig.4(b), or alternately in Fig.5(b). The peak of higher frequency turns into a double peak whose maximum values $\Delta P^{\rm r}_{32}(f)$ and frequency locations are respectively, (1.046, 0.66 Hz) and (0.8294,

0.6 Hz). Another peak value of $\Delta P^{\mathrm{r}}_{32}(f)$ (0.8203) at 0.42 Hz lies in a frequency area that has a lower energy than that of short wave train 2 (0.46 Hz). The result of nonlinear action of short wave train 3 on short wave train 2 is that the wave train energy sharply increases within a narrow frequency bandwidth whose frequencies are near the frequency of short wave train 2. This occurs at the price of wave train energy dissipation within a narrow frequency bandwidth whose frequencies are mainly near 0.38 Hz and 0.58 Hz.

The nonlinear sea surface whereby short wave trains ride on a long wave, and Fig.4, imply that we can obtain the mechanism of the nonlinear interactions between one short wave train and another. Specifically, one short wave train (expressed as wave train 2) leads to the energy focusing of the other short wave train (wave train 3) and this occurs for the wave components within a narrow frequency bandwidth whose frequencies are near the primary frequency of wave train 3. The same result can be obtained when the effects of nonlinear interactions of wave train 3 on wave train 2 are considered.

Comparing the peak value of $\Delta P^{\mathrm{r}}_{23}(f)$ in Fig.4(a) with that of $\Delta P^{\mathrm{r}}_{32}(f)$ in Fig.4(b), one finds that the maxima of $\Delta P^{\mathrm{r}}_{23}(f)$ are much larger than those of $\Delta P^{\mathrm{r}}_{32}(f)$. We may regard the energy of the first short wave train, which rides on the long wave, as perturbation energy. Thus, the other short wave train is being perturbed. In our example, the amplitudes of short wave train 2 and short wave train 3 are 0.09 m and 0.02 m, respectively. This means that the energy of short wave train 2 is much larger than that of short wave train 3. In Fig.4(a), short wave 2 acts on short wave train 3. The perturbation energy is much larger than the energy of the wave train that is being perturbed, which is exactly opposite to the situation for the case of Fig.4(b). In addition, we can consider the relative change in spectral intensity to the wave train that is being perturbed. Thus, as a general conclusion, the spectral intensity change is large, when a relatively low energy wave train is being perturbed by a high energy wave train as described by the example in Fig.4(a). Moreover, in the opposite case, the spectral intensity change is considerably smaller, when a relatively high energy wave train is perturbed by a low energy wave train as illustrated in Fig.4(b).

4. Summary

In this work, we present a novel numerical method to study the nonlinear interactions between a long wave and multiple short waves.

A given wave can be considered to be a 'nonlinear long wave' when a short wave or several short waves ride on the long wave. Frequencies, amplitudes and wave numbers of these nonlinear long waves are regarded as variable in time and space. They can also be considered to be discrete. The surface elevation of the nonlinear long wave at a certain point can be regarded as the corresponding surface elevation of a sine wave whose amplitude and wave–number equal those of the nonlinear long wave at the same point. Discrete interactions between the nonlinear long wave and the short wave are also assumed. The result of the interactions between the nonlinear long wave and short waves can be regarded as the sum of interactions between short waves and different sine waves whose amplitudes and wave–numbers are equal to those of the nonlinear long wave at different points. Thus, we derive formulae for amplitude and wave number modulations between long and short waves, and these are used to calculate the nonlinear evolution of the sea surface.

In obtaining these results, we show that our method is a useful tool for studying nonlinear wave–wave interactions. Our method can be used not only in oceanography (deep and shallow water cases), but also in other subjects which involve nonlinear wave–wave interactions such as the problems related to the study of electromagnetic scattering from the sea surface.

Another important application of our method is to quantitatively analyse the nonlinear interactions between one arbitrary short wave train and another short wave train. From numerical simulation results, we suggest that the mechanism for the nonlinear interactions between one short wave train and another short wave train (expressed as wave train 2) leads to energy focusing of the other short wave train (expressed as wave train 3) occurring on the wave components with a narrow frequency bandwidth whose frequencies are near the primary frequency of wave train 3.

References

[1] Chow C C, Bers A and Ram A K 1992 *Phys. Rev. Lett.* **68** 3379

[2] Phillips O M 1960 *J. Fluid Mech.* **9** 193

[3] Zakharov V E 1968 *Journal of Applied Mechanics and Technical Physics* **9** 190

[4] Dyachenko A I Lvov Y V and Zakharov V E 1995 *Physica* D **87** 233
[5] Lin R Q and Will Perrie, 1997 *J. Phys. Oceanography* **27** 2169
[6] Lvov Y V 1997 *Phys. Lett.* A **230** 38
[7] Sirendaoerji and Taogetusang 2006 *Acta Phys. Sin.* **55** 13 (in Chinese)
[8] Michael Stiassnie and Lev Shemer 2005 *Wave Motion* **41** 307
[9] Chen G and Belcher S E 2000 *J. Phys. Oceanography* **30** 2246
[10] Chen L X and Zhang J 1998 *Ocean Eng.* **125** 395
[11] Chen X G, Guo Z P and Song J B 2008 *Chin. Phys.* **17** B 3387
[12] Soomere T and Engelbrecht 2006 *J. Eur. J. Mech. B/Fluids* **25** 636
[13] Sedletsky Y V 2008 *J. Phys.* A **41** 035502
[14] Lo E and Chiang C M 1985 *J. Fluid Mech.* **150** 395
[15] West B J, Bruechner K A and Janda R S 1987 *J. Geophys. Res.* **92** 11803
[16] Tanos E, Thompson D R, Charpron B and Douglas V 2001 *Proc. R. Soc. Lond.* A **457** 2585
[17] Pan G D and Johnson J T 2006 *IEEE Trans. Geosciences and Remote Sensing* **44** 2880
[18] Sriram V, Sannasiraj S S and Sundar V 2006 *J. Fluid and Structures* **22** 663
[19] Ning D Z, Teng B, Taylor R E and Zang J 2008 *Ocean Eng.* **35** 887
[20] Unna P J 1941 *Nature* (London) **148** 226
[21] Unna P J 1942 *Nature* (London) **149** 219
[22] Unna P J 1947 *Nature* (London) **159** 239
[23] Longuet-Higgins M S and Stewart R W 1960 *J. Fluid Mech.* **8** 565
[24] Agnon Y, Sheremet A, Gonsalves J and Stiassnie 1993 *Coastal Engineering* **20** 29
[25] Berizzi F, Mese E D and Pinelli G 1999 *IEE Proc. Radar, Sonar Navig.* **146** 55
[26] Alves J H G M , Banner M L and Young I R 2003 *J. Phys. Oceanography* **33** 1301
[27] Pierson W J and Moskowitz L 1964 *J. Geophys. Res.* **69** 5181
[28] Hasselmann K, Barnett TP, Bouws E, Carlson H et.al. 1973 *Ergänzungsheft zur Deutschen Hydrographischen Zeits.* **12** Reihe A8 95